Correlated quantum percolation in the lowest Landau level

Nancy Sandler*
Department of Physics and Astronomy, Ohio University, Ohio 45701, USA

Hamid R. Maei†
Gatsby Unit, University College London, London, United Kingdom

Jané Kondev‡
Department of Physics, Brandeis University, Waltham, Massachusetts 02454, USA
(Received 20 November 2003; revised manuscript received 9 March 2004; published 15 July 2004)

Our understanding of localization in the integer quantum Hall effect is informed by a combination of semiclassical models and percolation theory. Motivated by the effect of correlations on classical percolation we study numerically electron localization in the lowest Landau level in the presence of a power-law correlated disorder potential. Careful comparisons between classical and quantum dynamics suggest that the extended Harris criterion is applicable in the quantum case. This leads to a prediction of localization quantum critical points in integer quantum Hall systems with power-law correlated disorder potentials. We demonstrate the stability of these critical points to addition of competing short-range disorder potentials, and discuss possible experimental realizations.

DOI: 10.1103/PhysRevB.70.045309 PACS number(s): 73.43.Nq, 64.60.Ak, 71.30.+h

I. INTRODUCTION

One of the hallmarks of the quantum Hall effect is the appearance of plateaus in the Hall resistance of a two-dimensional electron gas as a function of applied magnetic field. Transitions between plateaus have been associated with a quantum critical point.[1] This critical point corresponds to a localization-delocalization transition for the electron's wave function. Unlike the Anderson metal-insulator transition here the transition is between two insulating states: extended wave functions emerge at a single value of the magnetic field corresponding to the center of a Landau band. Experiments and numerical simulations have revealed many important properties of this critical point,[2] such as the value of the correlation length exponent, $\nu_q \approx 2.3$. Attempts at formulating an analytically tractable theory of the transition have by and large failed.

A very fruitful approach to unraveling the physics of plateau transitions has been the semiclassical description of electron dynamics in the lowest Landau level.[3] Classically the electron's motion can be described as a fast cyclotron rotation in the plane accompanied by a slow $\mathbf{E}\times\mathbf{B}$ drift of the center of the circular orbit along lines of constant random potential, $V(\mathbf{x})=\text{const}$. Quantum mechanics adds tunneling and interference to the mix.

The purpose of this work is to understand the relation between classical and quantum dynamics of electrons in the lowest Landau level, in the presence of a random potential. In particular we investigate the effect of the fractal geometry of the classical orbits on the critical properties of the quantum localization-delocalization transition, such as the value of ν_q. One of our main results is that we have identified a family of random potentials for which the classical electron orbits have continuously varying fractal properties, while the quantum critical point remains unchanged. These random potentials are characterized by decaying power-law correlations in space. When the decay of correlations is not too fast we find quantum critical points which are the quantum analogs of correlated percolation.[4]

Previously, a real-space renormalization group treatment of correlated quantum percolation appeared in Ref. 5. Preliminary results of our numerical approach were reported in Ref. 6. Here we provide a detailed account of the numerical methods used to study the effect of power-law correlated disorder potentials on the integer quantum Hall transition (IQHT), as well as theoretical arguments supporting them. We also describe results on the stability of these quantum critical points to the presence of short-range correlated disorder. The stability analysis provides connections with experiments[7] where these quantum critical points might be observed.

The work presented here addresses two different aspects of the problem. On one side motivation is provided by the role of disorder in determining the transport properties of quantum Hall systems. On the other side, we are motivated by the possibility of extending classical correlated percolation to the quantum regime.

A. Disorder and the quantum Hall effect

The role of disorder in the quantum Hall effect was recognized shortly after its discovery. From scaling theory it is known that electron wave functions are localized by potential disorder in two dimensions.[8] This remains true in the presence of a strong perpendicular magnetic field for states in the tails of the Landau bands, and leads to the observed plateaus in the Hall resistance.[9] Toward the center of a Landau band the localization length increases signaling the appearance of delocalized states. This results in the observed transition between plateaus in the Hall resistance and the peak in the longitudinal resistance.

The precise nature of the disordered potential experienced by electrons in quantum Hall systems remains poorly understood. The canonical picture (say, for GaAs heterostructures) is that ionized donors located between the two-dimensional electron gas and the sample surface are responsible for the random potential. Important experimental progress has come from scanning techniques which provide a map of the electrostatic potential seen by electrons in a semiconductor heterostructure.[10] Interestingly enough the experiment measures random potential fluctuations that extend over distances that are more than 1 order of magnitude larger than the typical spacing between the impurities and the electron gas, suggesting that the potential might be longer ranged that previously thought. Scanning techniques and the ability to manipulate single atoms on surfaces also opens up the possibility of engineering the random potential so as to produce specifically designed transport effects. For example, an enhancement of the conductivity (compared to the Drude value) of a two-dimensional electron gas was observed in Ref. 7 due to the presence of a random magnetic field. In this case the random field was produced by a thin film of rough magnetic material brought into close proximity to the electron gas. The fluctuations of the field were inherited from the height fluctuations of the film surface.

Inspired by these experimental advances here we describe how power-law correlated disorder can lead to exotic critical behavior of the electron gas in the integer quantum Hall setting. We also analyze the effect of competing disorders, which are necessarily present in semiconductor heterostructures, on the stability of these critical points.

B. Quantum percolation

The classical percolation problem provides one of the most intuitive examples of a critical point. Lattice sites are occupied with some probability p. Nearest neighboring sites, which are occupied, form clusters with a typical size ξ. As p is tuned to its critical value p_c, which depends on the lattice type, the correlation length ξ diverges as $\xi \sim |p_c - p|^{-\nu_c}$. ν_c is the correlation length exponent, and in two dimensions $\nu_c = 4/3$ independent of the lattice type.[11]

An analogous picture has been put forward to describe the localization transition in the integer quantum Hall system.[3] For a smooth random potential (one that varies little on the scale of the magnetic length) the electron wave function is localized along the level lines. For random potential symmetric around $V=0$ level lines away from the zero level are closed and have a typical size ξ, which is identified with the localization length. As the electron's energy is tuned to the center of the Landau band, the corresponding level line approaches $V=0$ and ξ diverges. If the random potential has short range correlations in space this is precisely the classical percolation problem[12] and one would predict a localization length exponent $\nu_q = \nu_c = 4/3$.

Experiments that measure a localization length exponent in the integer quantum Hall system find $\nu_q \approx 2.3$, signaling a breakdown of the simple percolation picture. The essential physics that has been left out is one of electron tunneling, which readily occurs at the saddle points of the random potential, as well as quantum interference. This was beautifully demonstrated by Chalker and Coddington, who proposed a lattice model which takes into account these purely quantum effects, by describing electron dynamics as hopping from one saddle point to the next with scattering matrices associated with each saddle.[13] The saddle points themselves occupy the vertexes of a square lattice. Computer measurements of the localization exponent for this model yield values in agreement with the experimental results. Moreover, taking a classical limit of the network model, in which the scattering matrices become classical probabilities for the two possible outcomes of a scattering event at a vertex, leads to classical percolation and a localization length exponent of $4/3$.[14] This provides an intriguing connection between the critical points of classical and quantum percolation. Here we investigate the nature of this connection when power-law correlations are introduced in the random potential. In the classical case it was shown that this can lead to different critical points if the power-law decay is not too fast. We show that a similar effect occurs for the quantum version of percolation provided by electron localization in the lowest Landau level.

The paper is organized as follows. In Sec. II we discuss the physics of classical and quantum electron motion in two dimensions, in the presence of a disordered potential and a strong perpendicular magnetic field. We present scaling arguments that show how the value of the critical exponent ν can be extracted from the time dependent mean square displacement (classical motion) and the time dependent wave-packet spread (quantum motion). In Sec. III we describe in detail the numerical methods used to obtain the value of ν in the classical and quantum setting. As evidence for the suitability of these methods, we present results for short-range correlated disorder potentials that are in good quantitative agreement with previous experimental and theoretical works.[2,13,14] Section IV contains the numerical results obtained for classical and quantum electron motion in power-law correlated disorder potentials. In Sec. V we propose a framework based on the classical Harris criterion[15] and its extension[16] that provides the theoretical support for our numerical results.

Finally, in Sec. VI we present results on classical and quantum localization in the presence of competing short-range and power-law correlated disorders. In experiments,[7] which we believe have a good chance of observing the quantum critical points discovered, both types of disordered potentials are present. The key question here is whether correlated quantum percolation is stable to the addition of short-range correlated disorder.

II. CLASSICAL AND QUANTUM MOTION IN THE LOWEST LANDAU LEVEL

The methods and tools used to describe the localization-delocalization transition in the lowest Landau level (LLL) in the classical regime are considerably different from the ones used in the quantum regime. In this section, we review both scenarios and present the arguments leading to the connection between the localization exponent ν and electron dynamics.

A. Classical motion

The two-dimensional semiclassical motion of an electron in a disorder potential under the influence of a large constant magnetic field (along the $\hat{z}$ axis), is described by the drift motion of the electron's guiding center along equipotential lines:

$$\frac{d\mathbf{r}}{dt} = \frac{c}{eB} \nabla V(\mathbf{r}) \times \hat{z}; \tag{1}$$

where $\mathbf{r}$ is the position vector for the guiding center in the $(\hat{x},\hat{y})$ plane. This equation is derived in the adiabatic approximation, i.e., under the assumption that the cyclotron radius is much smaller than the typical distance over which the potential changes.[17] Therefore the localization-delocalization transition in the LLL in the classical regime implies the study and characterization of the trajectories determined by this equation.

Equation (1) was extensively studied in two different albeit related contexts. Evers[18] used this equation in numerical studies of classical motion along the hulls of percolation clusters. He demonstrated interesting scaling behavior of the time-dependent density-density correlation function close to the percolation critical point.

Gurarie and Zee[19] arrived at Eq. (1) from the classical limit of the Liouvillian equation of motion for electrons in the lowest Landau level of the integer quantum Hall regime. In both cases, the authors considered smooth random potentials with short-range correlations in space.

One goal of this work is to study numerically properties of closed trajectories determined by Eq. (1), where $V(\mathbf{r})$ is power-law correlated in space. In particular, we focus on the scaling law, and its associated critical exponent ν, which describes how the size of a closed trajectory grows as the energy approaches its critical value.

To make explicit the connection between ν and the dynamics of a particle moving in a two-dimensional random potential, let us briefly review the argument presented in Ref. 19. For a fixed constant value of $V(\mathbf{r})=V_0$, there is a set of equipotentials associated with closed electron trajectories. These trajectories are the outer boundaries (hulls) of percolation clusters, with the occupation probability p of the percolation problem determined by V_0. In particular, the critical value of $p_c=1/2$ corresponds to $V_0=0$ in the units chosen. Several studies[18–20] have shown that the mean squared displacement between two points on a given trajectory $\Delta\mathbf{r}^2$ ($\mathbf{r}$ is the position vector for the particle on the trajectory), when averaged over all trajectories for fixed V_0, follows a diffusive law:

$$\langle \Delta\mathbf{r}^2(t)\rangle_{V_0} = D\ t \quad (t \ll t^*). \tag{2}$$

Here t^* is a characteristic time that depends on V_0.

Away from the percolation critical point particle trajectories are closed, and in the long-time limit the mean squared displacement reaches a constant value

$$\langle \Delta\mathbf{r}^2(t)\rangle_{V_0} = \xi^2 \quad (t \gg t^*), \tag{3}$$

where $\xi(V_0)$ is the localization length.

These considerations lead to a scaling form (at fixed V_0) for the mean squared displacement

$$\langle \Delta\mathbf{r}^2(t)\rangle_{V_0} = D\ t\ f\left(\frac{Dt}{\xi^2}\right), \tag{4}$$

where f is a scaling function. The classical result from percolation theory[20] for the correlation length, $\xi \propto |p-p_c|^{-\nu_c}$, leads to the expression $\xi \propto V_0^{-\nu_c}$, which in turn implies

$$\langle \Delta\mathbf{r}^2(t)\rangle_{V_0} = D\ t\ f\left(\frac{D\ t}{V_0^{-2\nu_c}}\right). \tag{5}$$

Finally, by averaging this equation over all values of V_0 one obtains the scaling relation

$$\overline{\langle \Delta\mathbf{r}^2(t)\rangle} \sim t^{\theta}, \tag{6}$$

where $\theta = 1 - 1/2\nu_c$ is the anomalous diffusion exponent. From simulations $\overline{\langle \Delta\mathbf{r}^2(t)\rangle}$ can be computed, which leads to a value for θ and, via the scaling relation just derived, to a value for the localization length exponent ν_c in the classical regime.

B. Quantum motion

One approach to study the localization-delocalization transition in disordered quantum systems is based on the different contributions that extended and localized electron wave functions make to the frequency dependent electrical conductivity.[21] Localized states appear in the electrical conductivity through the retarded density-density Green's function, a quantity that has an intuitive interpretation when written in terms of wave functions. When the electron is represented by a localized wave packet at position $\mathbf{r}$ and time $t=0$, the Green's function gives the value of the wave packet spread at time t. Since this wave packet describes the probability of finding the electron at a given position and time, its spread is a measure of the uncertainty of the electron's position, and as such it is an indicator of localization.

In most studies of localization, the Green's function is calculated in the momentum-frequency domain and studied in detail in the limit of large momenta or small frequency.[2,22] The purpose of this section is to show explicitly how the critical exponent ν_q can be extracted from the Green's function using instead the real time domain, as proposed by Sinova *et al.*[23]

Within this approach, one studies the disorder averaged density-density correlation function projected onto the LLL, i.e., the focus is on the unconstrained spectral function. As pointed out in Ref. 19, the applicability of the method rests upon the assumption that delocalized states in the IQH transition are isolated from each other and located at the centers of the Landau bands. Thus, when the density-density correlation function is restricted to one Landau level (the lowest being considered for simplicity), the contribution of delocalized states in that level dominates the sum over states in the small (q,ω) limit. Equivalently, the integral of the spectral function over all energies is dominated by the contribution from the critical energy in that limit. For our purposes, the main advantage of this approach is that it clearly spells out a

numerical scheme for studying the effect of power-law correlated disorder potentials on localization in the lowest Landau level.

In order to make connections with electron motion in the classical regime and also to fix the notation used in the rest of the paper, we review some of the main points of the approach.

Consider $2d$ spinless electrons (the electron spin is fixed by the magnetic field) in the x-y plane, under the combined effects of a magnetic field $\mathbf{B}=B\hat{z}$, perpendicular to the plane and a random potential $V(\mathbf{r})$ due to the presence of impurities. The electron-impurity interaction is given by

$$H=\sum_{\mathbf{k}} V_{-\mathbf{k}}\,\rho_{\mathbf{k}}, \tag{7}$$

where $\rho_{\mathbf{k}}=e^{i\mathbf{k}\cdot\mathbf{r}}$ is the one-particle density operator and $V_{\mathbf{k}}$ is the Fourier transform of the disorder potential. At high enough magnetic fields (or low enough temperatures), the kinetic energy is quenched to the value of the lowest Landau band and the sum is reduced to a sum over states in the LLL. Let $\overline{H}$ and $\overline{\rho}$ be the Hamiltonian and one-particle density operator projected onto the LLL. Then,

$$\overline{H}=\sum_{\mathbf{k}} V_{-\mathbf{k}}\,\overline{\rho_{\mathbf{k}}}, \tag{8}$$

with the projected one-particle density operator taking the form:

$$\overline{\rho_{\mathbf{k}}}=e^{-\ell_c^2\mathbf{k}^2/4}e^{i\mathbf{k}\cdot\mathbf{C}} \tag{9}$$

with $\mathbf{C}$, the position vector for the guiding center of a one-particle orbit, defined as[24]

$$C_x=x-\frac{c}{eB}\Pi_y,$$

$$C_y=y+\frac{c}{eB}\Pi_x, \tag{10}$$

and $\ell_c^2=\hbar c/eB$. Here $\mathbf{\Pi}=\mathbf{p}+(e/c)\mathbf{A}$ and (x,y) are the canonical momentum and position operators for one particle.

The formalism used to project the density operator $\rho_{\mathbf{q}}=e^{-i\mathbf{q}\cdot\mathbf{r}}$ onto the LLL was developed in Refs. 25 and 26. There it was shown that the commutation relation for the projected density operator obeys a closed algebra (the magnetic translation operator algebra):

$$[\overline{\rho_{\mathbf{k}}},\overline{\rho_{\mathbf{q}}}]=2\,i\,\sin\left(\frac{\ell_c^2}{2}k\times q\right)\times e^{(-\ell_c^2/2)\mathbf{q}\cdot\mathbf{k}}\rho_{\mathbf{k}+\mathbf{q}}, \tag{11}$$

with $k\times q=(\mathbf{k}\times\mathbf{q})\cdot\hat{z}$. This property implies that the equation of motion for the density operator

$$\imath\,\hbar\frac{\partial}{\partial t}\overline{\rho}=[\overline{H},\overline{\rho}] \tag{12}$$

is closed and can, in principle, be solved exactly.

Following the same line of argument, one can show that similar results also hold for the correlation function of the projected density operator:

$$G(\mathbf{r},t)=\mathrm{Tr}(\overline{\rho}(\mathbf{r},t)\overline{\rho}(\mathbf{0},0)). \tag{13}$$

Note that the trace extends over states in the lowest Landau level only. The density-density correlation function G in $\mathbf{k}$ space satisfies the equation[23]

$$\imath\,\hbar\frac{\partial}{\partial t}G(\mathbf{k},t)=\sum_{\mathbf{q}} 2\,i\,\sin\left(\frac{\ell_c^2}{2}k\times q\right)V(\mathbf{k}-\mathbf{q})\times\exp\left[-\frac{\ell_c^2}{2}(\mathbf{k}^2-\mathbf{k}\cdot\mathbf{q})\right]G(\mathbf{q},t), \tag{14}$$

which follows from Eq. (11). This is a Schröedinger-like equation where the effective Hamiltonian is the Liouvillian matrix:

$$\mathcal{L}_{\mathbf{kq}}=2\,\imath\,\sin\left(\frac{\ell_c^2}{2}k\times q\right)\,V(\mathbf{k}-\mathbf{q})\exp\left[-\frac{\ell_c^2}{2}(k^2-\mathbf{k}\cdot\mathbf{q})\right]. \tag{15}$$

The name Liouvillian is used because of the analogy with the Liouvillian operator in classical mechanics. Actually, the procedure outlined here reduces to the study of the time evolution of the width of a wave packet made with all localized and delocalized states which has been employed previously.[27,28]

An interesting feature of Eq. (14) is that for a fixed value of the magnetic field, the magnetic length $\ell_c(\ell_c^2=\hbar c/eB)$ vanishes in the classical limit $\hbar\to 0$. In units of $c/eB=1$, Eq. (14) gives[19]

$$\frac{\partial}{\partial t}G(\mathbf{r},t)=\epsilon_{ij}\partial_i V(\mathbf{r})\partial_j G(\mathbf{r},t). \tag{16}$$

A solution of this equation is $G(r,t)=\delta(\mathbf{r}-\mathbf{r}(t))$ where

$$\frac{d\mathbf{r}}{dt}=\nabla V(x,y)\times\hat{z}. \tag{17}$$

In other words, Eq. (16) describes the classical motion of the electron's guiding center along equipotentials of $V(\mathbf{r})$.[24]

As argued above, the Liouvillian driving the quantum dynamics of an electron in the LLL contains information about localization and the value of the critical exponent ν_q. The following scaling argument provides a numerical algorithm for extracting the localization exponent from the time dependent projected density-density correlation function. (We would like to draw attention to a close analogy between the present argument and the ideas presented in Sec. II A)

Let us start with Eq. (8), and assume that all eigenvalues and eigenstates, localized and delocalized, are known. We construct a wave packet at time $t=0$ using only localized states with energies in the Δ neighborhood $E'\neq 0$, and then we let the wave packet evolve in time. The state vector corresponding to such wave packets is

$$|\psi_{E'}(t)\rangle=\sum_i c_i(t)|i\rangle \tag{18}$$

where $|i\rangle$ are eigenvectors of the Hamiltonian projected onto the LLL [see Eq. (8)]. The sum runs over all (localized) states with energies within the range $[E'-\Delta,E'+\Delta]$.

At very short times, the spread of the wave packet as a function of time is ballistic (see Appendix for derivation). However, after some crossover time and before the localization length corresponding to the energy E' is reached, the spread of the wave packet averaged over disorder realizations is diffusive:

$$\overline{<\Delta r^2(t)>_{E'}} = D\ t \quad (t \ll t^*(E')). \tag{19}$$

At times much longer than $t^* \sim \xi^2$, the localization length is reached and

$$\overline{<\Delta r^2(t)>_{E'}} = \xi^2(E') \quad (t \gg t^*(E')). \tag{20}$$

In close analogy with the classical argument, a scaling form for the average dispersion of the wave packet follows:

$$\overline{<\Delta r^2(t)>_{E'}} = D\ t\ f'\left(\frac{D\ t}{\xi^2(E')}\right), \tag{21}$$

where f' is the appropriate scaling function. Now, if a localized wave packet at time $t=0$ is constructed with all the eigenstates (including delocalized states at the center of the LLL), its wave vector can be written as:

$$|\psi(t)\rangle = \sum_{E'} |\psi_{E'}(t)\rangle, \tag{22}$$

where the sum runs over all states with energies in the range $(-\infty, 0]$. The dispersion of the wave packet can be computed as

$$\overline{\langle \Delta r^2(t)\rangle} = \sum_{E',E''} \overline{\langle \psi_{E''}(t)|\Delta r^2|\psi_{E'}(t)\rangle}, \tag{23}$$

Using this decomposition:

$$\overline{\langle \Delta r^2(t)\rangle} = \sum_i \sum_j c_i^*(0)c_j(0)e^{i(E_i-E_j)t}\langle i|x^2|j\rangle, \tag{24}$$

where the sums run over all the eigenvectors of the Hamiltonian. For a fixed (and sufficiently large) time $t=t^*$, there are two different contributions to this expression: one coming from the states with energies within a range $\Delta E' \leqslant t^*/\hbar$ with slowly time-varying phases and the other coming from the rest of the states with much faster phase variations. Thus, for a given time t^* a window of states, close to the critical one, is selected. The contribution of this set of states will dominate over the other term due to phase randomization, and Eq. (23) can be approximated by

$$\overline{\langle \Delta r^2(t)\rangle} \simeq \int_{-\infty}^{0} dE' g(E')\langle \Delta \overline{r^2(t)}\rangle_{E'}, \tag{25}$$

where $g(E')$ is the density of states. Replacing $\langle \Delta \overline{r^2(t)}\rangle_{E'}$ by Eq. (21), using the fact that the density of states is nonsingular, and that ξ is related to E' by $\xi(E') \sim (E')^{-\nu_q}$, we obtain

$$\overline{\langle \Delta r^2(t)\rangle} \simeq \int_{-\infty}^{0} dE'\ g(E')D\ t\ f'\left(\frac{Dt}{E'^{-2\nu_q}}\right). \tag{26}$$

Finally, an appropriate rescaling gives

$$\overline{\langle \Delta r^2(t)\rangle} \sim t^{\theta}; \quad \theta = 1 - 1/2\,\nu_q, \tag{27}$$

and we conclude, as in the classical case, that the spread of the wave packet is subdiffusive with an anomalous diffusion exponent θ.

Therefore, by computing $\overline{\langle \Delta r^2(t)\rangle}$, the value of ν can be obtained. An alternative derivation of this result has been proposed in Ref. 29, where the energy integrated Liouvillian propagator is analyzed in the finite (q,ω) regime and the limits of $q \to 0$ and small ω are taken.

III. SHORT-RANGE DISORDER POTENTIAL

We introduce next the numerical procedures used to calculate the value of the critical exponent ν. We do this first in the case of a short-range correlated disorder potential, where we test the effectiveness of these numerical techniques by rederiving previously known results. We begin by introducing the method used for analyzing classical localization, where the connection to percolation theory provides a testing ground for our numerics. In Sec. III B we describe how the Liouvillian approach is implemented following the method introduced in Ref. 30 to analyze quantum localization. The numerical values thus obtained compare favorably to experimental results and previous numerical calculations.

A. Classical motion

To study the classical motion of the electron's guiding center along the equipotentials of $V(\mathbf{r})$ we make use of a lattice model, used previously to compute geometrical exponents for contour loops of rough interfaces.[31]

Consider a square lattice $\mathcal{L}$ with N sites and periodic boundary conditions. Each site in the lattice has assigned to it a random number that represents the value of the disorder potential $V(\mathbf{r})$ at that point in space. Its dual lattice $\mathcal{L}^*$ is the set of points that describe the positions of the electron in this potential landscape. Thus, an electron originally located at a site $\mathbf{r}_0$ of $\mathcal{L}^*$ will move along a path that joins points on this lattice. The trajectories are contour loops of the disorder potential. They are generated by first randomly selecting the initial position $\mathbf{r}_0$ from the set of points in $\mathcal{L}^*$. The choice of the initial position of the trajectory also fixes the value of the level V_0. V_0 is computed as the average of the values for $V(\mathbf{r})$ at the four vertexes (sites in $\mathcal{L}$) that surround the initial position $\mathbf{r}_0$. Once V_0 is determined, all the lattice sites of $\mathcal{L}$ can be labeled by + or −, depending on whether they are at a potential higher or lower than V_0. The numerical algorithm updates the electron's position by selecting the bond on the dual lattice that connects the point $\mathbf{r}_0$ with one of its nearest neighbor points, with the additional property that it crosses a +− bond on the lattice $\mathcal{L}$. With this construction, the contour loop is a directed walk along the bonds of the dual lattice $\mathcal{L}^*$ that separates potentials lying above (below) V_0 on the inside (outside) of the loop (see Fig. 1).

At each step, the square of the displacement vector between the current and original positions on the dual lattice is calculated. The procedure is repeated for different starting points $\mathbf{r}_0$, and different disorder realizations. All the calcu-

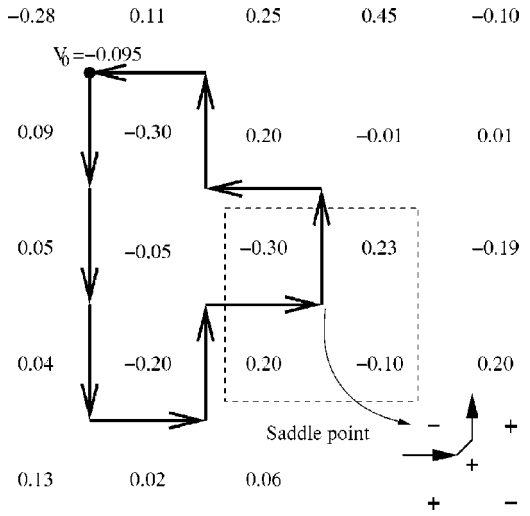

FIG. 1. Classical trajectory of the electron's guiding center, in the presence of a random potential whose values are indicated. V_0 is the average potential around the plaquette surrounding the initial point of the trajectory. The resolution of a saddle point is determined by the average potential around the plaquette surrounding the saddle.

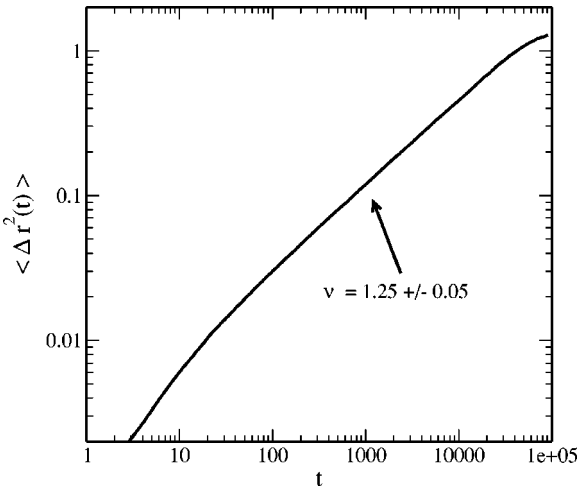

FIG. 2. Averaged mean square displacement for a classical particle drifting along equipotentials of a random short-range correlated potential. Distance is measured in units of lattice spacing and time in number of lattice steps. System size is 1024×1024. ν is related to the slope in the critical region θ, by $\theta=1-1/2\nu$.

lated quantities are averaged over all trajectories and over all disorder realizations.

A technical subtlety of this procedure is the existence of saddle-point plaquettes, with $+-+-$ labeled vertexes around them. In this case, two contours (four links) meet at the center and it is necessary to add an additional rule to resolve the connectivity, so as to convert this pattern into two 90° turns that are not quite touching. A physically sensible rule makes use of the average potential V_{plaq} of the four potentials around the saddle-point plaquette. If $V_{\text{plaq}}<V_0$, the center of the plaquette is at a lower potential than the contour loop and the connectivity is resolved by having the + sites inside the 90° turns. In the opposite case, $V_{\text{plaq}}>V_0$, the + sites are outside of the 90° turns (see Fig. 1).

As in Ref. 19 we find from simulations that the average time for an electron to traverse a certain distance on $\mathcal{L}^*$ is proportional to the distance. This observation justifies using the number of steps along $\mathcal{L}^*$ to measure the time elapsed. In this way time is rendered dimensionless.

The computations were carried out on two-dimensional square lattices with system sizes $N=256$, 512, and 1024. The values for the short-range correlated potential were chosen independently from site to site from a uniform distribution over the range $[-0.5,0.5]$. This choice leads to $V=0$ for the value of the critical equipotential energy. Figure 2 shows results for a 1024×1024 lattice obtained by averaging over 3×10^4 trajectories and 1000 different disorder realizations.

As discussed above, the diffusive (slope $\theta=1$), short-time ($t<t^*\sim10$), behavior is followed by a crossover to a critical regime where the value of the slope θ is a measure of the critical exponent ν_c; $\theta=1-1/2\nu_c$. By fitting the critical region to a line on a log-log graph we find

$$\nu_c = 1.25 \pm 0.05, \tag{28}$$

where the error bars reflect the uncertainty associated with choosing the critical region.

This value compares well with the exact result from percolation theory $\nu_c=4/3$.[11] The critical regime extends until finite size effects become dominant and $\langle\Delta r^2\rangle$ saturates, as observed in Fig. 2 for $t>2\times10^4$.

B. Quantum motion

Following the ideas presented in Sec. II B, we studied numerically the role played by quantum effects on electron dynamics in the lowest Landau level and in the presence of a short-range correlated random potential.

We use the approach proposed in Ref. 19 and use the eigenstates of the Hamiltonian for an electron on a torus geometry as the basis of states for the LLL. The corresponding wave functions written in the Landau gauge are:

$$\psi_\alpha(x,y) = \left[\sum_{m=-\infty}^{\infty} \exp\left(2\pi(x+\imath y)(N\,m+\alpha) - \frac{(Nm+\alpha)^2}{N}\pi\right)\right] e^{-\pi N x^2}, \tag{29}$$

where m takes integer values, N is the number of flux quanta through the torus, and the index α goes from 0 to $N-1$, labeling the N states in the LLL. These wave functions are periodic functions in the interval $(x,y)\in[0,1)\times[0,1)$, and are centered along narrow strips (of width ℓ_c) around the lines $x=\alpha/N$. In Eq. (29) (x,y) are dimensionless variables expressed in units in which the magnetic length is $\ell_c=1/2\pi N$.

The electron density operator $\rho(k_1,k_2)=\exp(2\pi i(k_1x+k_2y))$ projected onto the LLL using this basis, is a matrix of the form:

$$\overline{\rho}(k_1,k_2) = \exp\left(-\frac{k_1^2+k_2^2}{2N}\pi\right) L(k_1,k_2), \tag{30}$$

where k_1, k_2 are integers ($(k_1,k_2) \neq (0,0)$), and the matrix $L(k_1,k_2)$ is given in terms of two unitary unimodular $N \times N$ matrices:

$$L(k1,\, k2) = \epsilon^{k_1\, k_2/2} f^{k_1} h^{k_2},$$

$$h = \begin{pmatrix} 0 & 1 & ... & ... & 0 \\ 0 & 0 & 1 & ... & 0 \\ .... & ... & ... & ... & ... \\ 1 & 0 & ... & ... & 0 \end{pmatrix},$$

$$f = \mathrm{diag}(1, \epsilon, \ldots, \epsilon^{N-1}),$$

with $\epsilon = \exp(2\pi i/N)$; note that h is a cyclic permutation matrix. These matrices satisfy: $h\, f = \epsilon\, f\, h$ and $h^N = f^N = 1$. The explicit expression for the matrix elements of $L(k_1,k_2)$ is:

$$[L(k_1,k_2)]_{\alpha,\beta} = \epsilon^{k_1\, k_2/2 + k_1(\alpha-1)} \delta_{\alpha,\beta-k_2}|_{\mathrm{mod}\ N}. \tag{31}$$

Since the basis of states is restricted to the LLL, the kinetic energy is a constant and the projected Hamiltonian reduces to:

$$\overline{H} = \sum_{k_1,k_2} V(-k_1,-k_2)\overline{\rho}(k_1,k_2),$$

$$= \sum_{k_1,k_2} V(-k_1,-k_2)\exp\left(-\frac{k_1^2+k_2^2}{2N}\pi\right) L(k_1,k_2), \tag{32}$$

where the sum runs over all integer values of (k_1,k_2), and $V(0,0)=0$ (this choice amounts to fixing the critical energy at zero).

In this basis, the Hamiltonian is a random $N \times N$ matrix that can be diagonalized exactly. Notice that the projection operation introduces the exponential factor in Eq. (32) that effectively reduces the amplitude of the large (k_1,k_2) Fourier components of the potential (it acts as a soft large-momentum cutoff). The presence of this factor seems to indicate that the transition is driven by the small momenta components of the disorder potential. It is important to note that even when a finite precision numerical calculation fails to detect the contribution coming from momenta components higher than a maximum value for $(k_1^2+k_2^2)/2N$ (numerically, the Hamiltonian matrix becomes a banded matrix), it is incorrect to replace the exponential factor by a hard cutoff, since the commutation relations of the projected density operator[25] would not be conserved. (In numerical calculations, this translates into having results that are extremely sensitive to the value of the hard cutoff chosen.)

The values for the Fourier components of the disorder potential in Eq. (32) are chosen randomly from a flat distribution over the interval $[-0.5, 0.5]$.

We diagonalize the Hamiltonian to obtain all N eigenvalues and eigenfunctions. Figure 3 shows examples of a localized state at the tail of the Landau band, and a delocalized one close to the band center, obtained with a basis of $N = 1000$ states.

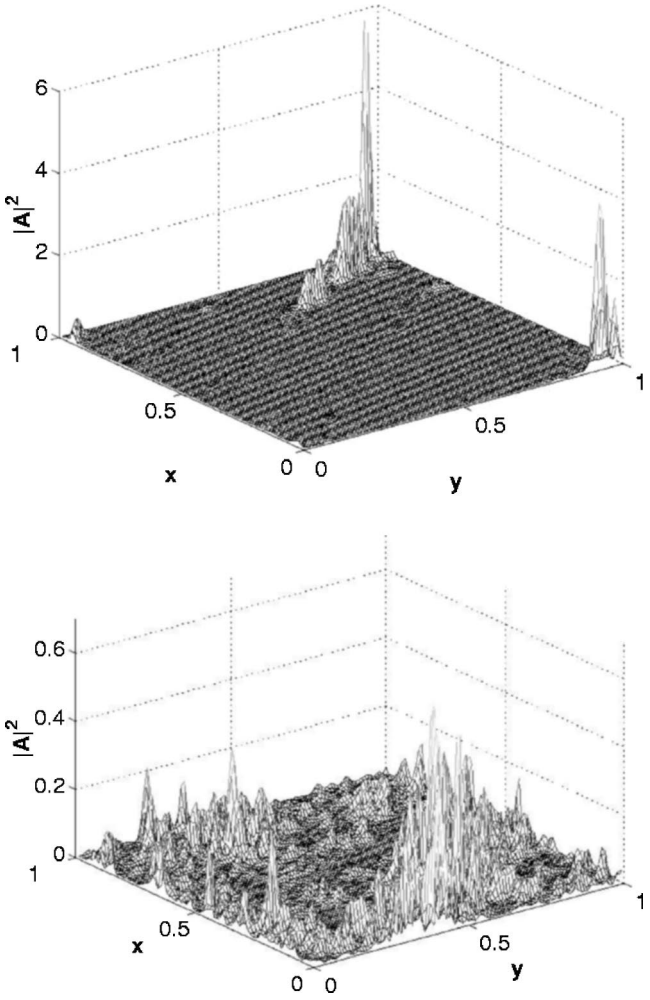

FIG. 3. Squared amplitude of a localized eigenstate with energy $E=9.6$ (top), and a delocalized one with $E=0.011$ (bottom), in the lowest Landau level with degeneracy $N=1000$. The disorder potential is short ranged.

A localized wave packet is constructed with all the eigenstates for a given disorder realization and, as it evolves, its spread is computed as a function of time. The wave packets are chosen from among the basis states, Eq. (29), which are localized in the x direction and completely spread out in the y direction (see Fig. 1 in Ref. 6). Thus, the contribution to the total spread from the y direction is a constant proportional to the system size.

The procedure is repeated for different initial positions for the localized wave packet and different disorder realizations. The spread is averaged over all initial positions and disorder realizations. A typical result for a basis of 1000 states and 1000 disorder realizations is plotted in Fig. 4.

As in the classical case, three regimes can be identified. For long enough times ($t>10$ in Fig. 4) the spread of the wave packet reaches a constant value, indicating the influence of the finite system size. The critical region corresponds to intermediate times ($0.4<t<10$), and the value of ν_q ("q" for quantum) can be related to the slope of the line, which is the anomalous diffusion exponent θ [see Eq. (27)]. As seen in the inset to Fig. 4, the slope in the critical region shows a

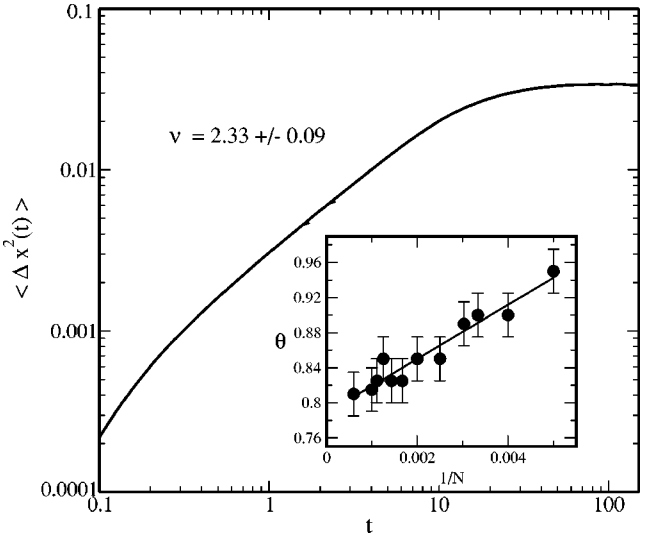

FIG. 4. Spread of wave packet as a function of time, in the presence of short-range correlated disorder potential with a basis of $N=1000$ states. The spread at intermediate times is subdiffusive. The inset shows the anomalous diffusion exponent θ as a function of basis size N. The intercept gives the infinite-system-size value of θ, which leads to the quoted value of the localization exponent $\nu(\nu=1/(2-2\theta))$.

strong dependence on the system size. To take into account these finite size effects, we determined the slope for systems sizes ranging from $N=200$ to $N=1500$ and compute the value for an infinite sized system by linear extrapolation to obtain $\nu_q=2.33\pm0.09$.

Our result compares favorably to the values measured in experiments $(\nu=2.3\pm0.1)$[32] and previous numerical simulations $(\nu=2.35\pm0.05)$.[2] This provides an important check on the numerical method.

Our data show that at very short times the slope $\theta\simeq2$, which implies ballistic spreading of the wave packet. In the Appendix we present a calculation based on perturbation theory that shows that this is a result of averaging the evolution equation over random disorder, at short enough times.

IV. POWER-LAW CORRELATED DISORDER POTENTIAL

In this section we address the central question raised by the present work: how does a change in the spatial correlations of the disorder potential affect the nature of localization in the lowest Landau level? The numerical procedure outlined in previous sections allows us to investigate this question in a straightforward manner, for both the classical and the quantum regime. Basically, it amounts to an appropriate modification of the probability distribution for the Fourier components for the random potential in Eq. (32). Since we are interested in the effect of power-law correlations on localization properties of the Hamiltonian in Eq. (32), the Fourier components are chosen independently with a Gaussian distribution with zero mean, and variance

$$\overline{|V(\mathbf{k})|^2} \propto 1/|\mathbf{k}|^{2-\alpha}. \tag{33}$$

Inverse Fourier transforming to real space leads to power-law correlations

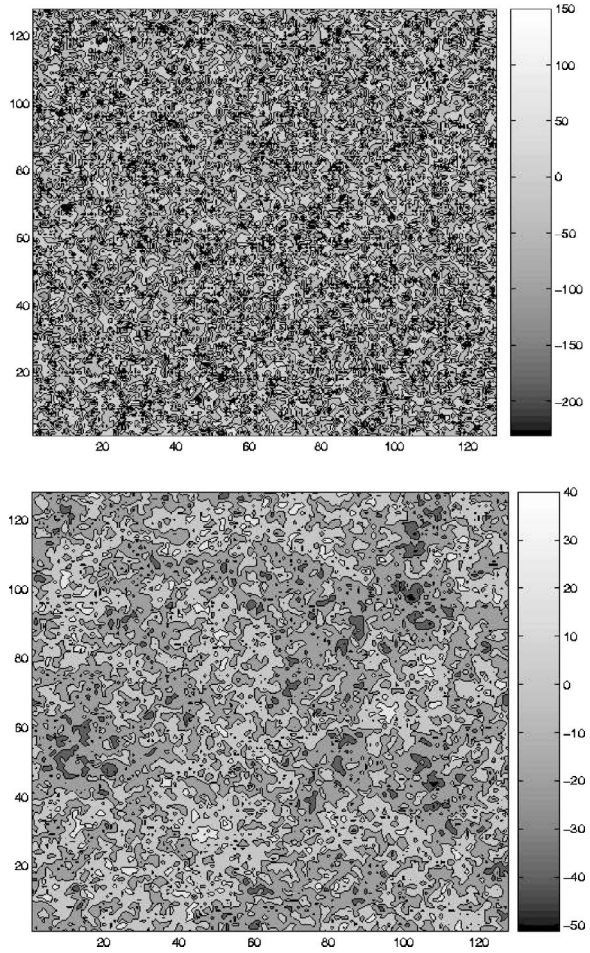

FIG. 5. Contour plot of a typical realization of a short-range correlated potential (top) and a power-law correlated one with exponent $\alpha=0.5$ (bottom).

$$\overline{V(\mathbf{r})V(0)} \sim 1/|\mathbf{r}|^{\alpha}. \tag{34}$$

The constant in Eq. (33) is fixed so that the variance of $V(r)$ is normalized to one. Long-range correlations strongly modify the real-space configuration of the equipotential lines as can be seen in Fig. 5 where a comparison between a short-range and a power-law correlated potential with $\alpha=0.5$ is given.

A. Classical motion

In the classical limit of the IQH transition, the effect of power-law correlations in the disorder potential can be described in terms of a purely geometric effect: they change the fractal geometry of the equipotential contours modifying the electron's path, and correspondingly, the anomalous diffusion law for its mean squared displacement.

To study this regime numerically, we repeated the procedure described in Sec. III A, and computed $\langle\Delta\mathbf{r}^2(t)\rangle$ for values of α ranging from 0.33 to 1.8. Figure 6 shows the curves obtained for a system of 512×512 lattice sites. As in the case of short-range correlations, three regimes can be identified with the onset of each of them depending on the value of α. From the figure, a qualitative change in the spread of the

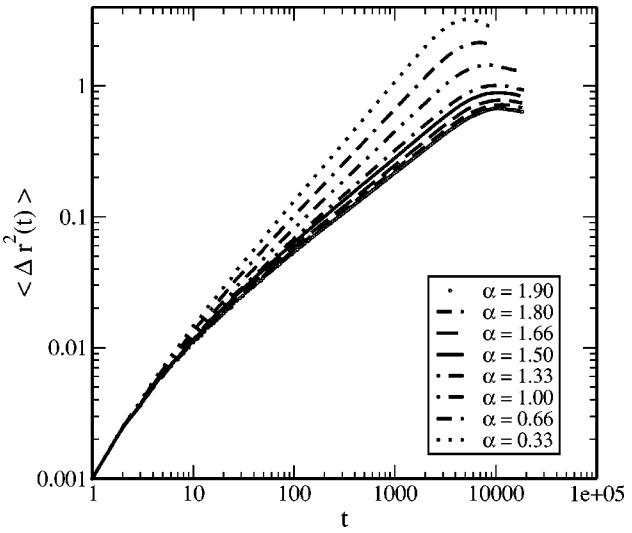

FIG. 6. Classical motion: averaged mean square displacement as a function of time for 512×512 system size. Distances are measured in units of lattice spacing and time in number of lattice steps.

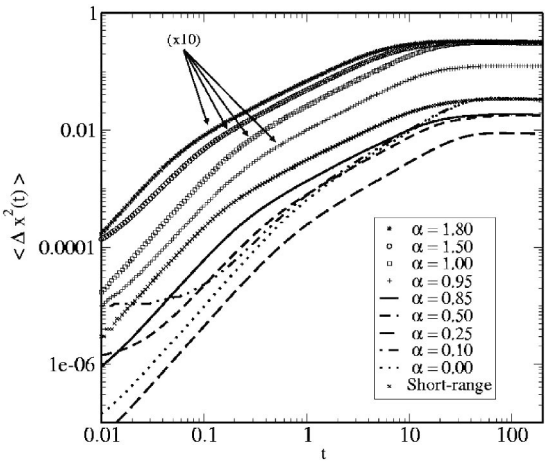

FIG. 7. $\overline{\langle \Delta x^2 \rangle}$ as a function of time for various values of the power-law correlated disorder exponent. Anomalous diffusion appears at intermediate times. The top four curves have been multiplied by a factor of 10 for clarity.

electrons position in time is observed. Namely, in the critical regime (typically for $30<t<1100$), the value of the slope becomes dependent on α when $\alpha\leqslant1.5$. As the value of α decreases (correlations increase) below a critical value of $\alpha_c^*\simeq1.5$ (c is for "classical"), the slope θ in the critical region increases and ν becomes an increasing function of α tending to infinity as α approaches zero.

B. Quantum motion

In contrast to the classical regime, the effect of power-law correlations in the disorder potential on the properties of quantum localization does not have a simple geometrical interpretation. In particular, we find that changing the fractal properties of the equipotentials does not always lead to a change in the quantum critical exponents.

The numerical procedure introduced in Sec. III B is easily extended to the present case allowing us to study the problem in detail. The Fourier components of the random potential are taken from the same distribution as in the classical case and the corresponding quantum Hamiltonian [Eq. (32)] is diagonalized. Then, $\overline{\langle \Delta x^2 \rangle}$ is computed as a function of time for values of α ranging from 0.1 to 1.9. A typical set of results obtained with a basis of 1000 states is shown in Fig. 7 together with the curve obtained for a short-range correlated potential. As in the short-range case, the exponent θ was calculated for different system sizes ranging from $N=300$ to $N=1000$.

As in the classical case, a qualitative difference in the slopes of the critical regime develops as α changes. A careful comparison among the different curves shows that the value of the slope in the critical region starts to increase below a critical value of $\alpha_q^*\simeq0.85$. A detailed quantitative analysis of these results together with a comparison to the classical case is the subject of Sec. V.

V. EXTENDED HARRIS CRITERION

The effect of a random disorder potential on the properties of continuous phase transitions in classical systems is summarized by the Harris criterion.[15] Basically, the criterion states that critical exponents of the disordered and the corresponding clean system remain equal as long as the value for the correlation length exponent ν satisfies the inequality: $d\nu-2\geqslant0$, where d is the dimensionality of the classical system under consideration. The criterion is derived by requiring that the variance of the thermodynamic quantity, which couples to the disorder within a volume set by the correlation length ξ, does not grow faster than its average value as the transition is approached and $\xi\rightarrow\infty$. The Harris criterion has been proven rigorously and generalized to a wider class of systems if an appropriate definition for the correlation length is adopted.[33] An extension of the criterion to power-law correlated disorder was proposed by Weinrib and Halperin.[16]

In the case of two-dimensional percolation with power-law correlations in the occupation probabilities, with the power-law exponent α, the extended Harris criterion states:

$$\alpha>\alpha_c^*=3/2 \quad \nu_c=\frac{4}{3},$$

$$\alpha<\alpha_c^*=3/2 \quad \nu_c=\frac{2}{\alpha}. \tag{35}$$

As a numerical check on Eq. (35), we computed the values of the anomalous diffusion exponent θ for classical electron motion. The values of θ were obtained from fitting the data in Fig. 6, in the critical region, to a line using a least-squares method; θ is the slope of the line. From θ we computed ν and plotted it as a function of α in Fig. 8. We see that the data are well described by the theoretical prediction: above $\alpha_c^*=3/2$, $1/\nu_c=2/3$ is constant, while below this value it varies as $1/\nu=\alpha/2$. Similar results were obtained previously by Prakash *et al.*[34]

Analogous results hold true for the quantum case; in Fig. 9 we plot $1/\nu$ as a function of α. The anomalous diffusion exponent θ was computed using the data in Fig. 7 and the value of $1/\nu$ was computed following the same procedure as

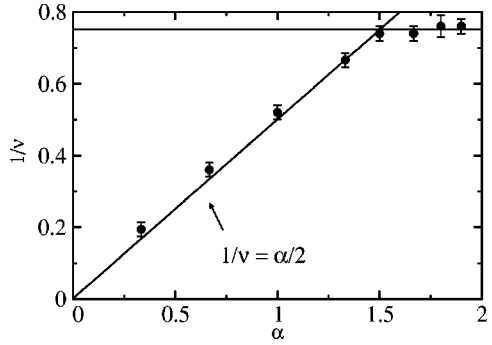

FIG. 8. Classical regime: inverse critical exponent $1/\nu$ as a function of power-law correlated disorder exponent α. The horizontal line represents the theoretical value of $1/\nu=0.75$ corresponding to the value of $\nu_c=4/3$ obtained from "classical" percolation theory. The linear function $1/\nu=\alpha/2$ is predicted by the extended Harris criterion, Eq. (35).

in the classical case. The values plotted are the extrapolation corresponding to an infinite system size. We see that the numerical results presented in Fig. 9 are in good agreement with the extended Harris criterion which now reads:

$$\alpha > \alpha_q^* \approx 0.85 \quad \nu_q \approx 2.33,$$

$$\alpha < \alpha_q^* \approx 0.85 \quad \nu_q = \frac{2}{\alpha}. \tag{36}$$

Support for the validity of the extended Harris criterion for quantum critical points was also provided by studies of quantum random magnets.[35]

In the case of quantum percolation (i.e., localization in the lowest Landau level) the extended Harris criterion can be argued for in close analogy to the classical case.[16] Namely, consider the average size of the fluctuations of the electron's energy in an area set by the localization length ξ. Like the electron's energy, it is also determined by the random disorder potential, and can be approximated as:

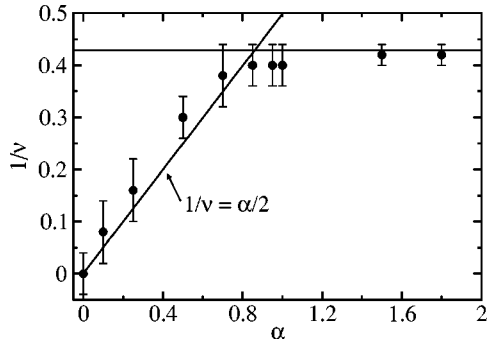

FIG. 9. Quantum regime: inverse critical exponent $1/\nu$ as a function of the exponent α, which determines the power-law correlations of the disorder. The lines are predictions of the extended Harris criterion [Eq. (36)] using the value $\nu_q=2.33$ for the quantum localization length exponent, in the case of short-range correlated disorder.

$$\overline{E^2} \approx \overline{\left(\frac{1}{\xi^2}\int_{\xi^2} d^2x V(\mathbf{x})\right)^2} \sim \frac{1}{\xi}\int_{\xi^2} d^2x |\mathbf{x}|^{-\alpha}, \tag{37}$$

where in deriving the second equation we have made use of $\langle V(\mathbf{x})V(\mathbf{x}')\rangle \sim 1/|\mathbf{x}-\mathbf{x}'|^{\alpha}$.

For the quantum critical point associated with localization in the lowest Landau level to be stable to the introduction of power-law correlations in the random potential, the fluctuations in the electron's energy should be small when compared to its energy E. Using Eq. (37), and the scaling relation $E \sim \xi^{-1/\nu}$ we arrive at the estimates

$$\frac{\overline{E^2}}{\overline{E^2}} \sim \begin{cases} E^{2\nu-2} & : \quad \alpha > 2 \\ E^{2\nu-2}\ln(E)^{-\nu} & : \quad \alpha = 2 \\ E^{\alpha\nu-2} & : \quad \alpha < 2. \end{cases} \tag{38}$$

The quantum percolation critical point is expected to be unaffected by the introduction of power-law correlations if $\overline{E^2}/E^2 \to 0$ when $E \to 0$, or, equivalently, when $\xi \to \infty$. Since $\nu > 1$ this is always the case when $\alpha \geqslant 2$.

However for $\alpha < 2$ there are two regimes to consider. When $2 > \alpha > 2/\nu$, $\overline{E^2}/E^2 \to 0$ and the localization critical point due to short-ranged potential disorder is again stable to introduction of power-law correlations in the random potential. In contrast, for values of $\alpha < 2/\nu$ a power-law correlated potential produces large fluctuations in the energy, thus destabilizing the critical point.

The usual expectation is that this relevant perturbation leads to a quantum critical point characterized by a value of ν. This is confirmed by our numerical results.

An important consequence of the present result regards the validity of the expression put forward in Ref. 36, that relates the values of ν_q and ν_c as follows:

$$\nu_q = \nu_c + 1. \tag{39}$$

According to the analysis presented above, a quantum system with a long-range correlated potential has the same critical exponent as one with short-range correlations as long as $\alpha \geqslant 0.85$. However, a classical system with potential correlations with a value for α in the region $0.85 < \alpha < 1.5$, has a continuously varying critical exponent ν according to Eq. (35). For instance, a value of $\alpha=1$ gives $\nu_q=2.33$, while $\nu_c=2.0$. This analysis suggests that the relation given by Eq. (39) (whatever the argument used to support it) is inconsistent with the Harris criterion.

VI. COMPETING DISORDERS

In this section we undertake a numerical study of the effect of competing disorders on localization in the LLL. We investigate first the classical regime, which is in the universality class of correlated percolation. Analytical calculations[4] have shown that in these systems the classical critical point generated by a long-range correlated potential is stable against perturbations produced by a short-range correlated potential. As shown below, our numerical results in this regime, provide support for this picture.

In the quantum case we investigate the effect of competing power-law correlated and short-range correlated disor-

TABLE I. Statistical properties of the short-range and long-range correlated potentials used in Sec. VI.

$V_{eff}(\mathbf{r})$	=	$\kappa\, V_s(\mathbf{r})+(1-\kappa)V_l(\mathbf{r})$
$\langle V_s(\mathbf{r})\rangle=\langle V_l(\mathbf{r})\rangle$	=	0
$\langle V_s^2(\mathbf{r})\rangle=\langle V_l^2(\mathbf{r})\rangle$	=	1
$\langle V_s(\mathbf{r})V_s(\mathbf{r}')\rangle$	$\propto$	$\lvert\mathbf{r}-\mathbf{r}'\rvert^{-\alpha}, \quad \delta(\mathbf{r}-\mathbf{r}')$
$\langle V_l(\mathbf{r})V_l(\mathbf{r}')\rangle$	$\propto$	$\lvert\mathbf{r}-\mathbf{r}'\rvert^{-\beta}$

ders on localization. Numerical studies of this particular case are relevant for experiments attempting to measure properties of the correlated quantum percolation critical point. Namely, since short-range correlated potentials are always present in experimental setups, it is important to understand quantitatively how their presence affects the values of the localization length exponents described in the previous sections.

To proceed with the appropriate numerical model we first establish the following conventions. The total disorder potential is defined as a weighted sum of two potentials: one with short-range correlations $V_s(\mathbf{r})$ and one with long-range correlations $V_l(\mathbf{r})$. The units chosen are such that the mean values of short- and long-range correlated potentials are set equal to zero while their variances are normalized to one. In this way, the maximum amplitudes of both potentials are comparable. In order to vary the relative strength of each potential we introduce a parameter κ with values in the range $0\leqslant\kappa\leqslant 1$ such that the total potential is:

$$V_{eff}(\mathbf{r}) = \kappa\, V_s(\mathbf{r}) + (1-\kappa)V_l(\mathbf{r}). \tag{40}$$

Note that when $\kappa=0$ the total potential has power-law correlations only, while the short-ranged part is increasingly dominant as the value of κ increases toward 1. This definition ensures that the variance of the total potential V_{eff} remains fixed as κ changes and $\langle V_{eff}^2(\mathbf{r})\rangle=1$.

The numerics were performed with short-range correlated potentials constructed from random Fourier components $V(\mathbf{k})$ sampled from a uniform distribution, or from a Gaussian distribution with variance $\sim|\mathbf{k}|^{\alpha-2}$ with $\alpha>\alpha^*$. In real space this leads to delta correlations and power-law correlations with exponent α, respectively. Long-range correlated potentials were generated with power-law correlations with exponent $\beta<\alpha^*$, for which the extended Harris criterion predicts a localization length exponent $\nu=2/\beta$. The properties of the total potential and its components are summarized in Table I.

A note on the evaluation of errors: as it will be shown in the following sections, the effect of tuning $\kappa\neq 0$ depends on system size for both classical and quantum regimes. Hence, it was not possible to carry out the finite-size study similar to the one done previously, where there is only one type of disorder present. As a consequence, the errors have been estimated from the largest systematic error involved in the procedure, which appears in the determination of the slope of the critical region.

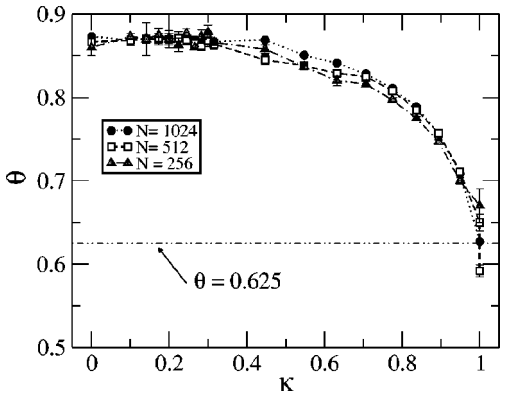

FIG. 10. Classical regime: slope θ as a function of parameter κ. $\kappa=0(1)$ indicates a pure long-range (short-range) correlated potential.

A. Classical regime

Computations were carried out for system sizes $N=256$, 512 and $N=1024$. The values of the anomalous diffusion exponent θ were extracted from the critical region of the spread of the classical position of the electron, as in Sec. IV A. Values of θ were obtained for a range of values of the parameter κ. Figure 10 shows result that correspond to a combination of a power-law correlated potential with exponent $\beta=0.5$ (for the long-range part) and $\alpha=1.8$ (for the short-range piece).

The figure shows that, as the system size increases the value of θ (and hence of ν) remains closer to the pure long-range value up to fairly large values of κ (roughly 55%–60%). The increasing sharpness of the crossover with increasing system sizes suggests a very sharp crossover in the thermodynamic limit. In the language of the renormalization group, this is an indication of the stability of the long-range critical point when perturbed with a short-range correlated potential. Notice, as it was pointed out above, that this crossover is strongly dependent on the system size, rendering useless the finite-size scaling analysis used previously. An interesting effect is observed in the raw data that points to the way the crossovers occur in finite size systems. Between the initial crossover from diffusive to subdiffusive motion and the final crossover from subdiffusive motion to saturation, there are two clearly distinguishable regimes. At the earlier times, the slope is determined by the short-range correlated potential. Only at the latest times (and before saturation effects dominate) does a new slope appear, that corresponds to the value of θ determined by the exponent of the power-law (long-range) correlated potential.

B. Quantum regime

In contrast to the classical regime, to date there is no experimental or theoretical work to our knowledge that attempted to investigate the influence of mixed long-range and short-range correlated disorder potentials on the integer quantum Hall transitions. The numerical strategy used in Sec. IV B, provides us with a framework to study this situation and allows us to examine the stability of the quantum critical points found in previous sections.

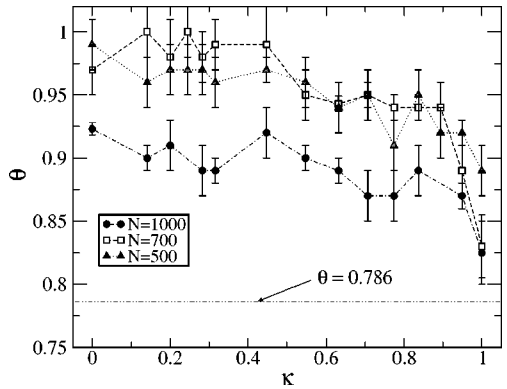

FIG. 11. Quantum regime: slope θ as a function of parameter κ. $\kappa=0$ indicates a purely long-range correlated potential and $\kappa=1$ corresponds to a purely short-range correlated potential.

Computations for quantum systems were carried out with a basis of $N=500$, 700, and $N=1000$ states. The values of the slope θ were extracted from the critical region and plotted as a function of the parameter κ, as in the classical regime. The results shown in Fig. 11 were obtained with power-law correlated potentials V_s and V_l with exponents $\alpha=1.8$ and $\beta=0.5$, respectively.

As the figure shows, data for the quantum regime is noisier than its classical counterpart. Finite size effects are also more prominent as can clearly be observed in the variation of the values of the slope θ. However, the trend observed is in agreement with the expected behavior in the thermodynamic limit. It suggests that the quantum correlated critical points are indeed stable against the perturbation introduced by a short-range correlated potential. This opens up the possibility of measuring the varying localization length exponents ν_q in experiments in which random disorder with power-law correlations is introduced. The idea would be to engineer a random potential with desired properties which would compete with the short-range disorder due to the impurities always present in the semiconductor heterostructure. An example of such a system was described in Ref. 7 where a thin magnetic film was placed in close proximity to the two-dimensional electron gas resulting in a random magnetic field. By controlling the height fluctuations of the film one can, in principle, engineer a random potential with desired correlations.

VII. CONCLUSIONS

We have analyzed the effect of spatial correlations of the disorder potential on the localization-delocalization transition in the integer quantum Hall system. The main purpose of the analysis was to understand separately the role played by quantum effects and disorder on the critical properties of the transition by comparing classical and quantum localization.

The analysis of electron localization in the classical case reveals that the localization length exponent is completely determined by the statistical properties of the level lines of the random potential. Using the tools of percolation theory, we were able to implement well established numerical methods to perform a detailed check of the validity of the Harris criterion. We found numerical support for the extended version of the criterion, confirming previous theoretical arguments.[4]

The quantum regime was analyzed by studying the real time density-density propagator as proposed in Ref. 23. This method, originally introduced as an alternative way to calculate the critical exponent ν for a short-range correlated potential, proved to be an excellent testing ground to analyze the role of disorder. We obtained (following a rather simplistic finite size analysis) a value for $\nu=2.33\pm0.09$ remarkably close to experimentally measured values and numerically calculated ones. We also found that when the decay of power-law correlations of the random potential is slow enough, this can destabilize the quantum critical point and lead to exotic critical behavior, as predicted by the extended Harris criterion.

Comparison between classical and quantum regimes with long-range correlated disorder potentials indicate that the effect of disorder correlations are qualitatively similar for quantum and classical systems. The main difference between these two cases seems to be the critical value of α (the exponent determining the long-range correlations) below which the value of ν is changed. The value of $\alpha_q^* \simeq 0.85$ is smaller compared to its classical counterpart $\alpha_c^*=1.5$. This suggests that quantum fluctuations can be thought of as effectively smearing out the correlations in the random potential, thus shifting α^*.

An immediate consequence of these results is that in the quantum case, there is no direct connection between the statistical properties of equipotential lines and the localization length exponent. Specifically, we were able to show that the fractal geometry of the equipotential lines can be continuously varied while the quantum localization length exponent does not change.

The detailed numerical study of the variation of the critical exponent ν with the power-law exponent α, led us to propose a precise statement for the quantum version of the extended Harris criterion. These numerical results are supported by a scaling argument, in close analogy with the classical case. Let us remark that previous works[37,38] have addressed the related issue of variable potential correlations on generalized Chalker-Coddington models to study the effect of classical percolation on the IQHT. In that case, however, it was concluded that the only effect was an increment of the microscopic length scale, with no further influence on the value of the critical exponents.

In order to address the experimentally relevant situation of samples with disorder potentials of different origins and likely, different correlations, we analyzed the effect of competing disorder potentials on the IQHT. In the classical limit, our numerical results give support to previous theoretical arguments for the stability of the correlated-percolation critical points. In the quantum regime we observed that, while the value of the critical exponent ν varies as the short-range correlated potential is introduced, the trend is similar to the one observed in the classical regime. As a consequence, our results show no qualitative difference between classical and quantum regimes regarding the stability of these critical points. More importantly, they point to the possibility of ob-

serving effects of the correlated quantum percolation critical points in experiments on two-dimensional electron gases in semiconductor heterostructures where short-range disorder due to impurities is unavoidable.

ACKNOWLEDGMENTS

It is a pleasure to acknowledge useful conversations with B. Halperin, J. Sinova, V. Gurarie, S. Boldyrev, J. Moore, H. Castillo, S. Simon, and G. Murthy. J.K. is supported by the NSF under Grant No. DMR-9984471, and is a Cottrell Scholar of Research Corporation.

APPENDIX

In this Appendix we present a calculation based on perturbation theory that shows that at short times the wave packet has a ballistic spread, as was observed numerically. If $|\psi(t)\rangle$ is the wave function of the wave packet at time t, the spread is given by

$$\langle\psi(t)|\Delta x^2|\psi(t)\rangle=\langle\psi(t)|x^2|\psi(t)\rangle-\langle\psi(t)|x|\psi(t)\rangle^2. \quad \text{(A1)}$$

Here we analyze the first term in detail, while the second one can be dealt with in a similar way.

In the Heisenberg representation

$$\langle\psi(t)|x^2|\psi(t)\rangle=\langle\psi(0)|x^2(t)|\psi(0)\rangle, \quad \text{(A2)}$$

where

$$x^2(t)=e^{iHt}x^2(0)e^{-iHt}. \quad \text{(A3)}$$

Using the well known operator identity

$$\langle\psi(t)|x^2|\psi(t)\rangle=\langle\psi(0)|x^2(0)|\psi(0)\rangle+i\,t\,\langle\psi(0)|[H,x^2(0)]|\psi(0)\rangle + \frac{(i\,t)2}{2!}\langle\psi(0)|[H,[H,x^2(0)]]|\psi(0)\rangle+\mathcal{O}(t^3). \quad \text{(A4)}$$

The probability distribution of energies is determined by the probability distribution of the disorder potential, which is chosen to be symmetric around the value $V=0$. Since the wave packet contains all eigenstates, averaging over disorder (average over energies) eliminates the linear term in the expansion above. Thus, the first nonvanishing contribution at short times is given by the quadratic term, which results in the ballistic spread of the wave packet.

*Electronic address: sandler@ohio.edu
†Electronic address: maei@brandeis.edu
‡Electronic address: kondev@brandeis.edu

[1] H. Levine, S. B. Libby, and A. M. M. Pruisken, Phys. Rev. Lett. **51**, 1915 (1983).
[2] B. Huckestein, Rev. Mod. Phys. **67**, 357 (1995), and references therein.
[3] S. A. Trugman, Phys. Rev. B **27**, 7539 (1983).
[4] A. Weinrib, Phys. Rev. B **29**, 387 (1984).
[5] P. Cain, R. A. Römer, M. Schreiber, and M. E. Raikh, Phys. Rev. B **64**, 235326 (2001).
[6] N. Sandler, H. Maei, and J. Kondev, Phys. Rev. B **68**, 205315 (2003).
[7] L. Zielinski, K. Chaltikian, K. Birnbaum, C. M. Marcus, K. Campman, and A. C. Gossard, Europhys. Lett. **42**, 73 (1998).
[8] E. Abrahams, P. Anderson, D. Licciardello, and T. Ramakrishnan, Phys. Rev. Lett. **42**, 673 (1979).
[9] R. Laughlin, Phys. Rev. B **23**, 5632 (1981).
[10] G. Finkelstein, P. Glicofirdis, R. Ashoori, and M. Shayegan, Science **289**, 90 (2000).
[11] M. P. M. den Nijs, J. Phys. A **12**, 1857 (1979).
[12] M. Isichenko, Rev. Mod. Phys. **64**, 961 (1992).
[13] J. T. Chalker and P. D. Coddington, J. Phys. C **21**, 2665 (1988).
[14] D.-H. Lee, Z. Wang, and S. A. Kivelson, Phys. Rev. Lett. **70**, 4130 (1993).
[15] A. B. Harris, J. Phys. C **7**, 1671 (1974).
[16] A. Weinrib and B. I. Halperin, Phys. Rev. B **27**, 413 (1983).
[17] T. G. Northrop, *The Adiabatic Motion of Charged Particles* (Wiley, New York, 1963).
[18] F. Evers, Phys. Rev. E **55**, 2321 (1997).
[19] V. Gurarie and A. Zee, Int. J. Mod. Phys. B **15**, 1225 (2001).
[20] R. M. Ziff, X. P. Kong, and E. G. D. Cohen, Phys. Rev. A **44**, 2410 (1991).
[21] D. J. Thouless, Phys. Rep., Phys. Lett. **13**, 93 (1974).
[22] J. T. Chalker and G. D. Daniell, Phys. Rev. Lett. **61**, 593 (1988).
[23] J. Sinova, V. Meden, and S. M. Girvin, Phys. Rev. B **62**, 2008 (2000).
[24] Z. F. Ezawa, *Quantum Hall Effects: Field Theoretical Approach and Related Topics* (World Scientific, Singapore, 2000).
[25] S. Girvin and T. Jach, Phys. Rev. B **29**, 5617 (1984).
[26] S. Girvin, in *Proceedings of Les Houches Summer School on Topological Aspects of Low Dimensional Systems, France 1998*, edited by A. Comtet, T. Jolicoer, S. Ouvry, and F. David (Springer, France, 2000).
[27] B. Huckestein and L. Schweitzer, Phys. Rev. Lett. **72**, 713 (1994).
[28] B. Huckestein and R. Klesse, Phys. Rev. B **59**, 9714 (1999).
[29] V. Oganesyan, J. T. Chalker, and S. L. Sondhi, Phys. Rev. B **68**, 045318 (2003).
[30] S. Boldyrev and V. Gurarie, J. Phys.: Condens. Matter **15**, L125 (2003); cond-mat/0009203.
[31] J. Kondev, D. Salinas, and C. Henley, Phys. Rev. E **61**, 104 (2000).
[32] S. Koch, R. J. Haug, K. von Klitzing, and K. Ploog, Phys. Rev. Lett. **67**, 883 (1993).
[33] J. T. Chayes, L. Chayes, D. S. Fisher, and T. Spencer, Phys. Rev. Lett. **57**, 2999 (1986).
[34] S. Prakash, A. Havlin, M. Schwartz, and H. E. Stanley, Phys. Rev. A **46**, R1724 (1992).
[35] H. Rieger and F. Iglói, Phys. Rev. Lett. **83**, 3741 (1999).
[36] G. V. Mil'nikov and I. M. Sokolov, JETP Lett. **48**, 536 (1989).
[37] R. Klesse and M. Metzler, Europhys. Lett. **32**, 229 (1995).
[38] M. Metzler, J. Phys. Soc. Jpn. **68**, 144 (1999).